Quasi-classical trajectory study of the stereodynamics of a Ne+H_2^+ →NeH^++H reaction*

Ge Mei-Hua(葛美华)† and Zheng Yu-Jun(郑雨军)

School of Physics, Shandong University, Jinan 250100, *China*

(Received 19 February 2011; revised manuscript received 21 March 2011)

We have carried out a quasi-classical trajectory calculation for the reaction of $Ne + H_2^+$ ($\nu = 0, j = 1$) → $NeH^+ + H$ on the ground state ($1^2A'$) using the LZHH potential energy surface constructed by Lü *et al.* [Lü S J, Zhang P Y, Han K L and He G Z 2010 *J. Chem. Phys.* **132** 014303]. Differential cross sections at many collision energies indicate that the reaction is dominated by forward-scattering. In addition, the NeH^+ product shows rotationally hot and vibrationally cold distributions. Stereodynamical results indicate that the products are strongly polarized in the direction perpendicular to the scattering plane and that the products rotate mainly in planes parallel to the scattering plane.

Keywords: quasi-classical trajectory, stereodynamics, product vibrational distribution, product rotational distribution

PACS: 34.50.Lf, 82.20.Kh, 82.20.Pm **DOI:** 10.1088/1674-1056/20/8/083401

1. Introduction

Recently, atom–molecule ion reactions and the related systems have attracted much attention[1,2] since they can play an important role in many interesting cases including interstellar processes, electric discharges and planetary ionospheres. Rare gas-hydrogen systems have continued to provide an important insight into chemical reaction dynamics. So Ne+H_2^+ →NeH^++H reaction has been the subject of numerous experimental[3−7] and theoretical[4,8−19] studies.

In order to obtain accurate potential energy surfaces (PESs) for the title reaction, many efforts have been made.[8,15−19] There are also many dynamical calculations in order to calculate reaction probabilities,[8−14,17] integral cross sections (ICSs)[4,9−13,16] and product rotational distributions (PRDs),[11] and so on. Almost all these dynamical calculations[9−14] are based on the same analytical PES in Ref. [15], while the initial rotational state ($j = 0$) and collision energies for these calculations are different from those in Refs. [4] and [8]. Recently, Lü *et al.*[8] presented a new LZHH PES for the ground state ($1^2A'$) of the title reaction from accurate *ab initio* data and carried out an exact quantum scattering study as well. The well in their PES[8] is 0.026 eV deeper (when the Ne–H–H angle is 180°) and the energy barrier is 0.075 eV (when the Ne–H–H angle is 90°) lower than the corresponding ones of Ref. [15]. Their calculated cross sections including Coriolis coupling (CC) fit well with the experimental ones.[4] However, a relatively large difference exists between the corrected quasi-classical trajectory (QCT) cross sections of Zhang *et al.*[4] and those of the quantum mechanical (QM) calculation.[8] There is a discrepancy between their CC ICSs and the results of previous studies.[4,9−13,16] Lü *et al.*[8] assumed that the difference was ascribed to the use of different PESs.

According to selection rules for homonuclear molecules, transition from excitation states with odd (or even) rotational quantum numbers to the rovibrational state of $\nu = 0$, and $j = 0$ (or $j = 1$) is forbidden. So only transition between two odd (or even) rotational states is allowed. Lü *et al.*[8] and Zhang *et al.*[4] considered the initial rotational state as $j = 1$ in the QM calculation and experimental study, respectively. So one can find that it is necessary to study the dynamical characteristics of the $\nu = 0$ and $j = 1$ state. As exhibited in Ref. [20], the characteristic of a potential energy surface could be evaluated in classical trajectory calculations. The QCT method constitutes a good approximation to the scattering dynamical properties and the qualification of a dynam-

*Project supported by the National Natural Science Foundation of China (Grant No. 21073110) and the Independent Innovation Foundation of Shandong University of China (Grant No. 10000059614011).

†Corresponding author. E-mail: mhge@sdu.edu.cn

© 2011 Chinese Physical Society and IOP Publishing Ltd

ical feature as a quantum effect in a given reactive system requires the performance of QCT calculations on the same PES. So we present a quasi-classical calculation of $Ne + H_2^+ \rightarrow NeH^+ + H$ on the $1^2A'$ PES given by Lü *et al.*[8] with the initial state of H_2^+ at $\nu = 0$ and $j = 1$ so as to testify whether the disparity between the results of Lü *et al.* and those of former researchers lies in the difference between PESs. The total cross sections are calculated to compare with CC results of Lü *et al.*,[8] the experimental ICSs,[4] the fitted experimental results through the line-of-centre collision (LOC) model[4] and those of corrected QCT[4] as well. With the development of laser techniques, the accurate measurement of the reagent/product orientation and alignment in molecular reactions has become available. To rationalize experimental results, one needs the assistance of computational work. Generally, theoretical exploration on the stereodynamics falls into two categories: one is for those of reagent $\boldsymbol{k}-\boldsymbol{j}$, $\boldsymbol{j}-\boldsymbol{k}-\boldsymbol{k}'$ vector correlations and the other is for those of product $\boldsymbol{k}-\boldsymbol{j}'$, $\boldsymbol{k}-\boldsymbol{k}'-\boldsymbol{j}'$ vector correlations, where $\boldsymbol{k}/\boldsymbol{k}'$ and $\boldsymbol{j}/\boldsymbol{j}'$ denote the relative velocity vectors of reagent/product and the reagent/product rotational angular momentum in the centre of mass (CM) frame, respectively. Only limited theoretical calculations, using either quasi-classical trajectory methods, quantum scattering, wave packet propagation techniques or simple models,[21−34] have been made of angular momentum polarization. As far as we know, up to now few stereodynamical characteristics of the title reaction have been studied, so we provide some stereodynamical information about the product $\boldsymbol{k}-\boldsymbol{j}'$, $\boldsymbol{k}-\boldsymbol{k}'-\boldsymbol{j}'$ vector correlations. Differential cross sections (DCSs) as a function of both the scattering angle and collision energy are calculated, which exhibits the sensitivity of DCSs to the scattering angle and collision energy, and the tendency of scattering direction of NeH^+. There is also an exhibition of product vibrational and rotational distributions over the considered collision energy interval. In addition, he polar angular distribution, $P(\theta_r)$, the distribution of the dihedral angle denoting $\boldsymbol{k}-\boldsymbol{k}'-\boldsymbol{j}'$ correlation, $P(\phi_r)$ and the angular distribution of product rotational vectors in the form of polar plots $P(\theta_r, \phi_r)$ are calculated to validate more information about the angular momentum polarization and orientation.

2. Computational aspects

Our calculation is performed on $1^2A'$ PES presented by Lü *et al.*[8] As is shown in Fig. 1, there is a deep well in the collinear geometry and its depth decreases with Ne–H–H angle decreasing, and at some point the well turns into barrier. The barrier height is 0.425 eV in perpendicular geometry. The ground state surface has an overall minimum in collinear geometry and the well is about 0.536 eV deep with respect to the reaction asymptote. For the details of the PES, readers may refer to Ref. [8]. Based on classical

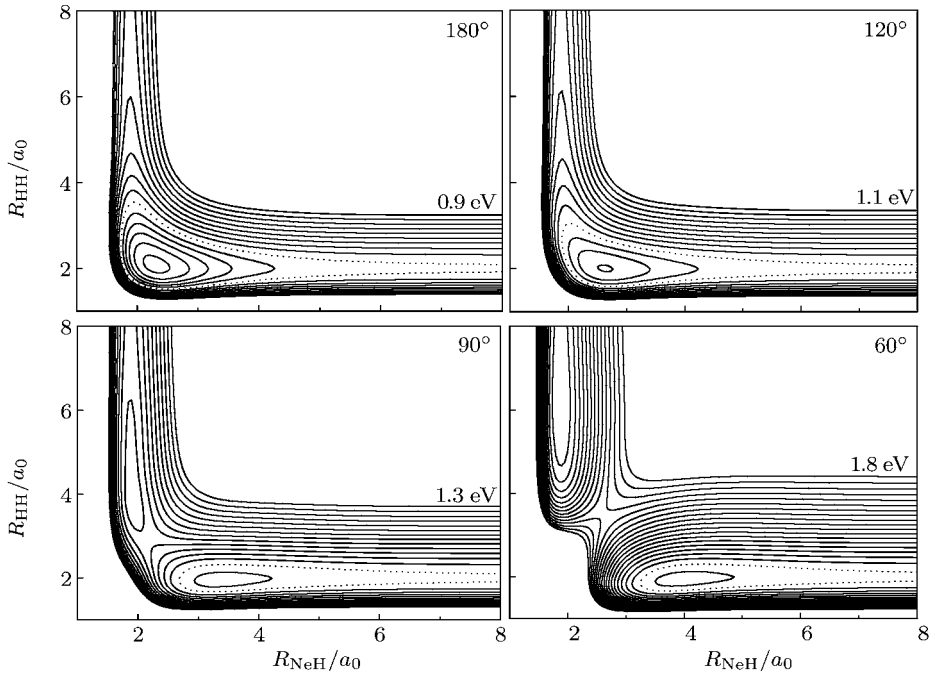


Fig. 1. Contour plots of the PES for the four different Ne–H–H angles in internal coordinates (180°, 120°, 90°, and 60°). The dotted line denotes 0 eV relative to the energy of the reactant Ne+ H_2^+.

trajectory method, in the QCT method some important quantum effects (using the vibrational and rotational quantum numbers to describe the reagent/product state) are taken into consideration, and the QCT method has been used to study the reaction dynamics of many systems. The calculation method we used is the same as the one described in Refs. [21]–[30].

In QCT calculation, there is uncertainty in determining the optimized impact parameter $b_{\max}$. The associated uncertainties with the QCT total cross section can be calculated by $\Delta\sigma = [(N_{\rm tot} - N_{\rm r})/(N_{\rm tot} \cdot N_{\rm r})]^{1/2}\sigma$. Therefore, we estimate the error margin for the present QCT ICS to be less than ±6.7%.

3. Results and discussion

The classical Hamilton equation is solved in three dimensions. We carry out the calculation with the initial vibrational and rotational numbers $\nu = 0$ and $j = 1$, respectively. The values of translational energy $E_{\rm col}$ range from 0.4 eV to 1.5 eV with the energy gap 0.1 eV. The time integral step size is chosen as 0.1 fs and 50000 trajectories are used in the computation.

In Fig. 2, our QCT ICSs and the associated errors are compared with previous results,[4,8] including quantum dynamical (CC) results, the experimental measurements, the deconvoluted LOC results (which are fitted to the ICS curve according to their experimental results by using the modified LOC threshold function) and corrected QCT results (which refers to proton transfer cross sections corrected for NeH+ products with vibrational energies below the zero point energy). Peaking at $E_{\rm col} = 1.0$ eV, our QCT ICSs display an increasing-then-decreasing trend over the whole collision energy range. For the CC and the experimental results, the phenomena are similar. Our calculated threshold is a bit smaller than that of CC computation and the deconvoluted one, owning to a well-known handicap of classical mechanics as zero point energy leakage.[35,36] Over the considered energy range, QCT ICSs are smaller than the experimental ones. The same situation also occurred in Ref. [13], which stated that the unusually large QCT cross sections at the threshold are mainly because of the inability of classical mechanics to handle correctly the zero-point energy of the products and the smaller QCT cross sections at higher energies are due to a combination of tunneling processes and the existence of the resonances. So we ascribe the discrepancy to the neglect of quantum effect in the QCT calculation. Except for the case in Ref. [16], different initial ro-vibrational states are chosen for the ICS calculation, moreover, the authors used a different PES in Ref. [16], which might result in the discrepancy between the CC results of Lü *et al.* and previous results. The main difference between the PESs used in the present paper and that in Ref. [14] is the well depth and the energy barrier. The former PES[8] has a deeper well depth for collinear geometry and a lower energy barrier when the Ne–H–H angle is 90°. The differences are 0.06 eV and 0.115 eV, respectively. In a word, the magnitude and profile of present QCT ICSs accord well with the CC and experimental results compared with previous results. In addition, the smaller QCT ICSs at higher collision energies ($E_{\rm col} > 1.0$ eV) perhaps result from the large number of resonances (which could be observed in reaction probabilities of Lü *et al.*[8]) and tunneling processes (which might be ascribed to the deep well at large Ne–H–H angles).

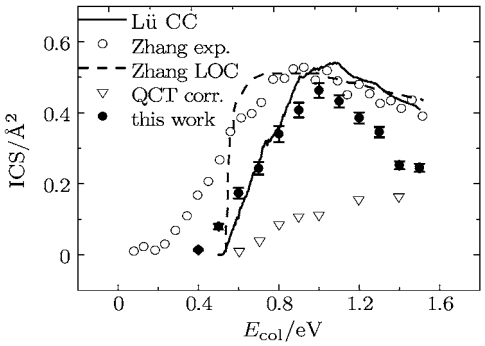


Fig. 2. Comparison between present ICSs (filled circles) and previous ones (CC of Lü *et al.* (solid line); experimental measurements of Zhang *et al.* (open circles); the deconvoluted LOC results (dashed line); and corrected QCT cross sections (open triangles). And the error bars (2.6%–6.7%) for the QCT ICSs represent the maximum absolute errors (1 Å=0.1 nm).

DCSs as a function of both the scattering angle (the angle between the reagent relative velocity $\boldsymbol{k}$ and the product velocity $\boldsymbol{k}'$) and collision energy $E_{\rm col}$ are given in Fig. 3 so as to explain the tendency of scattering direction of the product. For each of the considered energies there exists a maximum when the scattering angle θ_t is 36.9°, which suggests that the forward-reaction is dominant. The forward type distribution is consistent to a certain extent with

the experimental results in Ref. [7], which were obtained at $E_{\rm col} = 0.87$ eV (namely within the range of our translational energies). Due to the fact that the ro-vibrational states are not distinguished from the reagent states, a linear combination of all H_2^+ states (probably a Franck–Condon distribution) is applied to the experimental results. Their experimental measurements[7] result in a strong forward distribution. The agreement between our calculations and the experimental results is due to two reasons: (i) vibrational excitation greatly enhances reactivity,[8,11,12,17] and according to the results of Ref. [12], the DCSs of $\nu = 1$, 2 in their studied energy interval (which is within the energy range of our calculation) also demonstrate strong forward scattering; (ii) as expected, the contribution of all higher vibrational states will also be in the forward direction, as they all lead to exothermic reactions. From Fig. 3, one can observe that DCS is sensitive to the collision energy, especially for small scattering angle. Also DCS displays an increasing-then-decreasing trend over the whole collision energy range, and the peak appears at a collision energy of 1.0 eV, which is in accordance with the ICS result.

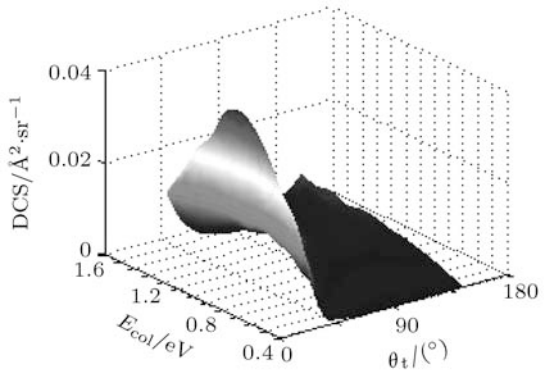


Fig. 3. DCSs as a function of both the scattering angle θ_t and collision energy $E_{\rm col}$ for the Ne + H_2^+ ($\nu = 0$, $j = 1$) $\rightarrow$ NeH^++H reaction.

The QCT method allows for a complete state-to-state study of the reaction dynamics, so we calculate the product vibrational and rotational distributions of NeH^+ as shown in Fig. 4. From Fig. 4(a), we find that only four product vibrational levels at the highest energies scanned here are open, and the product vibrational distributions (PVDs) all peak at $v' = 0$ over the whole energy range. In general, the lowest vibrational state is favoured and the distribution appears to be cold with a probability of zero above $v' = 3$. The main interesting point is that if the increased collision energy is not larger than the energy gap between two vibrational states of the reagent, the number of the vibrational channel to be open would not increase, but it could have influence on the distribution function for a defined v', especially for small collision energies. For example, when the collision energy varies from 0.4 eV to 0.6 eV, the number of the open vibrational channel remains unchanged ($v' = 0$) with a distribution ratio 1:5.8:12.7 (from small to large collision energy).

Figure 4(b) exhibits the PRDs for the collision energies of 0.4 eV–1.5 eV. Overall PRDs demonstrate a unimodal distribution at almost all the collision energies, peaking at an intermediate value of the open product rotational quantum numbers. More scanned product rotational levels are open when the collision energy is increased. Another interesting feature exhibited in Fig. 4(b) is the dependence of PRD on collision energy. It is not the same for each collision energy. The most striking effect can be observed when the collision energy goes from 0.4 eV to 0.6 eV. We find that high states become more populated as the collision energy increases, yielding a distribution peaked at $j' = 1$ at 0.4 eV, $j' = 2$ at 0.5 eV, and $j' = 3$ at 0.6 eV, which implies that the peak shifts towards larger rotational quantum numbers with the increase of collision energy.

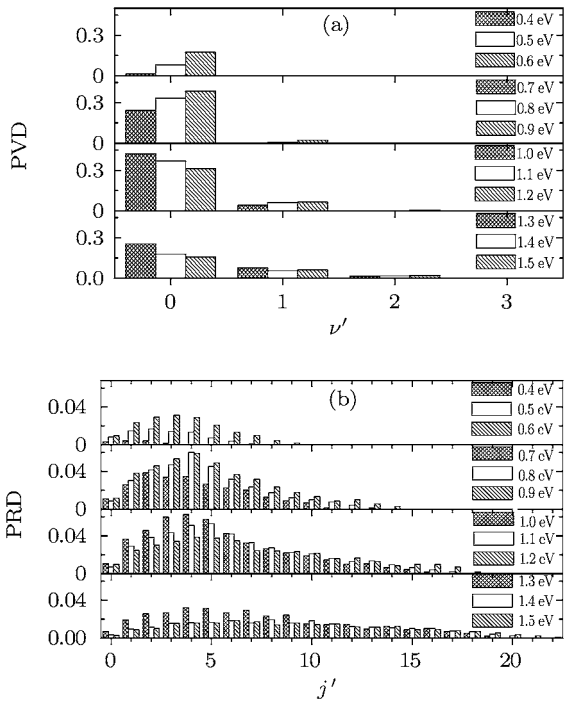


Fig. 4. Product ro-vibrational distributions for the Ne + H_2^+ ($\nu = 0$, $j = 1$) $\rightarrow$ NeH^+ (v', j') + H reaction: (a) PVDs, (b) PRDs.

The vibrational and the rotational excitations of the product exhibit different distribution functions. Through the comparison between Figs. 4(a) and 4(b), we can conclude that the NeH^+ product is rotationally hot and vibrationally cold. Owing to the large number resonances in reaction probabilities of Lü *et al.*,[8] the title reaction is dominated by the formation of a complex. As shown in Fig. 1, the deep well in the PES accounts for such a complex-forming scheme. The complex-forming mechanism usually favours the molecule rotating in various directions. As j' increases the rotational angular momentum becomes increasingly polarized. It might explain the wider range of product rotational population, and this assumption can be further testified through the depictions of $P(\theta_r)$ and $P(\phi_r)$ distributions in Figs. 5 and 6.

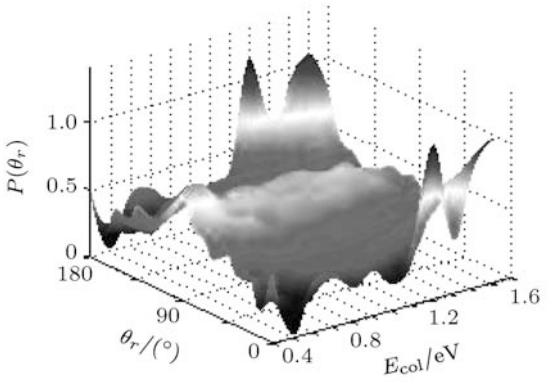


Fig. 5. The distribution of $P(\theta_r)$ as a function of both the polar angle θ_r and collision energy E_{col} for the reaction of $Ne + H_2^+$ ($\nu = 0$, $j = 1$) $\rightarrow$ $NeH^+ + H$.

To obtain a graphical representation of the polarization we plot the $P(\theta_r)$ distribution as a function of both the polar angle θ_r and collision energy E_{col} in Fig. 5. Obviously, there is a demonstration of symmetric distributions peaked at $\theta_r = 90^\circ$ over the whole energy range, implying that the product angular momentum tends to align in the direction perpendicular to $\boldsymbol{k}$. Since higher and narrower distribution indicates stronger product alignment, one can observe that the alignment degree is much larger at low collision energies (e.g. 0.4 eV and 0.5 eV) than that at higher collision energies. There is a non-monotonic relationship between the alignment degree and the collision energy. The structure of PES (with a deep well and a late barrier) might give a reason of such a phenomenon.

The $P(\phi_r)$ distributions are given in Fig. 6, which can provide some stereodynamical information about both the alignment and the orientation characteristics of the product. The ϕ_r denotes the azimuthal angle of the final rotational angular momentum $\boldsymbol{j'}$. All $P(\phi_r)$ distributions are asymmetric with respect to $\boldsymbol{k}$–$\boldsymbol{k'}$ plane (the scattering xz plane) with two peaks appearing nearly at $\phi_r = 90^\circ$ and $\phi_r = 270^\circ$, which demonstrates that $\boldsymbol{j'}$ is preferentially aligned along y axis. The larger peak existing nearly at $\phi_r = 90^\circ$ or $\phi_r = 270^\circ$ indicates a stronger product orientation along the positive or negative direction of y axis. It is interesting that the $P(\phi_r)$ distributions are asymmetric although the title reaction is symmetric about the initial relative velocity vector. Orientation of the product maybe results from the repulsive energy between the two atoms of H_2^+, which leads to the violation of the symmetry. Through comparison, we find that the orientations along the positive and the negative y axis coexist at the considered energy range, and the dominant $+y$ axis or $-y$ axis orientation appears at medium collision energies. Moreover, the direction and the degree of the alignment/orientation change with collision energy.

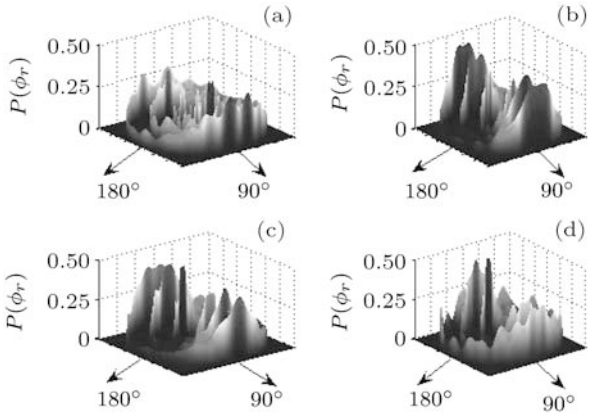


Fig. 6. The $P(\phi_r)$ distributions as a function of the dihedral angle ϕ_r at the collision energies of (a) 0.4, 0.5, 0.6 eV; (b) 0.7, 0.8, 0.9 eV; (c) 1.0, 1.1, 1.2 eV; and (d) 1.3, 1.4, 1.5 eV (from inner to outer) for $Ne + H_2^+$ ($\nu = 0$, $j = 1$) $\rightarrow$ $NeH^+ + H$ reaction.

To further examine the tendencies, we also plot the angular momentum polarization in the form of polar plots of θ_r and ϕ_r averaged over all scattering angles as shown in Fig. 7. The features of $P(\theta_r, \phi_r)$ distributions with peaks and valleys are in good accordance with those of the $P(\theta_r)$ and $P(\phi_r)$ distributions of the products. Also the depictions in Fig. 7 indicate that the products are strongly polarized in the direction perpendicular to the scattering plane (x–z plane is the scattering plane containing the initial and the final relative velocity vectors, $\boldsymbol{k}$ and $\boldsymbol{k'}$) and the products rotate mainly in planes parallel to the scattering plane.

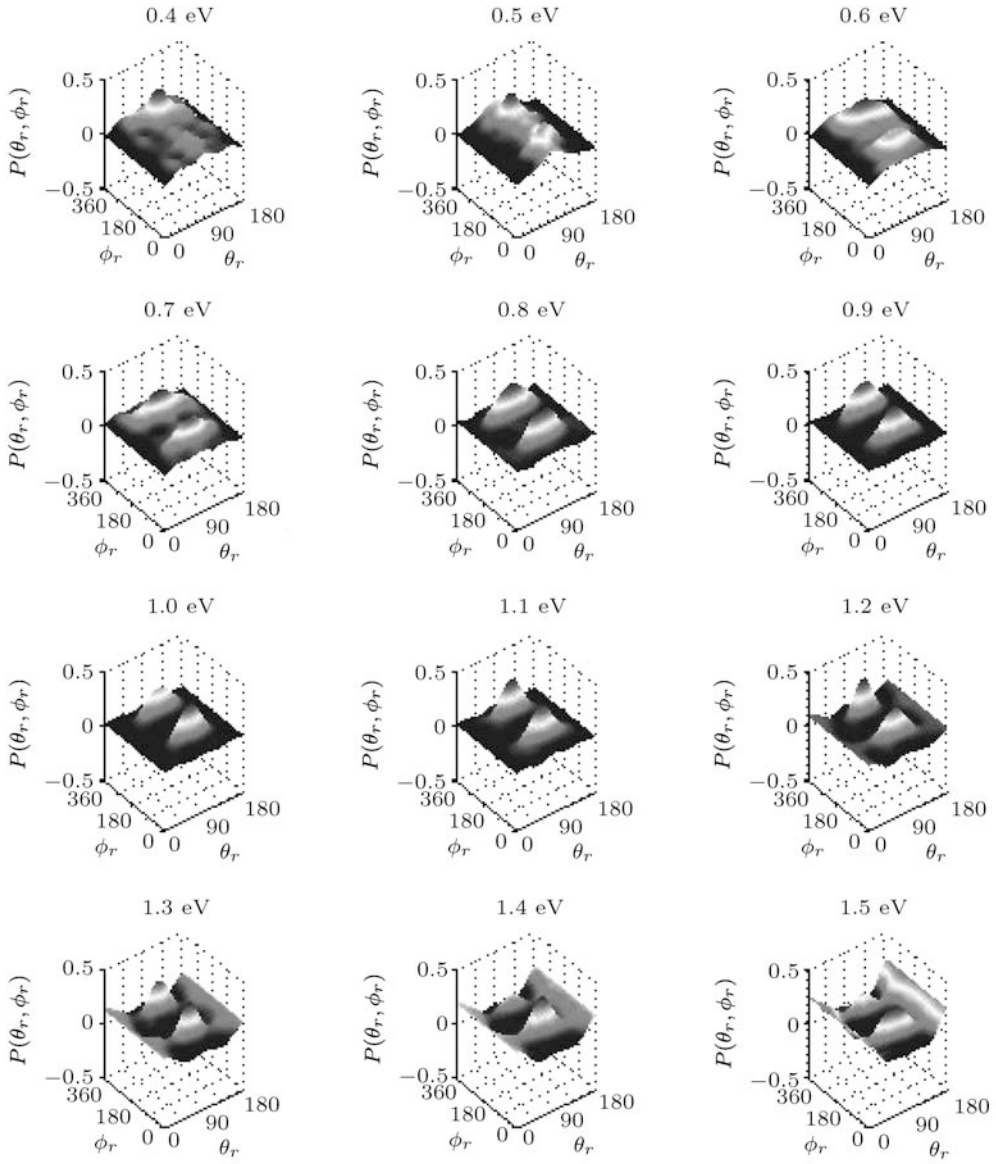


Fig. 7. Joint $P(\theta_r, \phi_r)$ distributions as a function of both polar angle θ_r and ϕ_r for the Ne + H_2^+ ($\nu = 0$, $j = 1$) → $NeH^+ + H$ reaction.

4. Conclusion

QCT calculation is performed to investigate dynamical information about the title reaction at the initial ro-vibrational state $\nu = 0$, and $j = 1$. Compared with previous results, the calculated cross sections are close to the accurate QM and experimental ones, which proves the validity of QCT calculation. According to our QCT results, the disagreement between the CC ICSs of Lü *et al.* and former results is probably due to employing different PESs and different initial states. DCSs as a function of both the scattering angle and translational energy are given, which manifests that the forward-scattering is dominant and DCS is not a monotonic function of collision energy. Also, the product vibrational and rotational distributions are computed. The product vibrational state population is rather cold (the lowest $v' = 0$ vibrational state of NeH^+ is favoured) and PRDs are highly selective (medium rotational numbers are favoured). Our results show a high rotational excitation in the product state distribution. Over the range of the considered collision energies, according to the vector properties of the title reaction, distribution $P(\theta_r)$ is symmetric with respect to 90°, and the dihedral angle distribution $P(\phi_r)$ manifests $\boldsymbol{j'}$ preferentially aligned along the y axis. Also the distributions of $P(\theta_r, \phi_r)$ showing the products rotate mainly

in planes parallel to the scattering plane are in good accordance with the distributions $P(\theta_r)$ and $P(\phi_r)$.

Acknowledgement

The authors are very grateful to Prof. Han Ke-Li for providing the computational codes and the potential energy surface.

References

[1] Chu T S and Han K L 2008 *Phys. Chem. Chem. Phys.* **10** 2431
[2] Chu T S, Zhang Y and Han K L 2006 *Int. Rev. Phys. Chem.* **25** 201
[3] Dressler R A, Chiu Y, Levandier D J, Tang X N, Hou Y, Chang C, Houchins C, Xu H and Ng C Y 2006 *J. Chem. Phys.* **125** 132306
[4] Zhang T, Qian X M, Tang X N, Ng C Y, Chiu Y, Levandier D J, Miller J S and Dressler R A 2003 *J. Chem. Phys.* **119** 10175, and references therein
[5] Herman Z and Koyano I 1987 *J. Chem. Soc. Faraday Trans.* **83** 127
[6] Van Pijkeren D, Boltjes E, Eck J V and Niehaus A 1984 *Chem. Phys.* **91** 293
[7] Bilotta R M and Farrar J M 1981 *J. Chem. Phys.* **75** 1776
[8] Lü S J, Zhang P Y, Han K L and He G Z 2010 *J. Chem. Phys.* **132** 014303
[9] Mayneris J, Sierra J D and González M 2008 *J. Chem. Phys.* **128** 194307
[10] Huarte-Larrañaga F, Giménez X, Lucas J M, Aguilar A and Launay J M 2000 *J. Phys. Chem.* A **104** 10227
[11] Huarte-Larrañaga F, Giménez X, Lucas J M, Aguilar A and Launay J M 1999 *Phys. Chem. Chem. Phys.* **1** 1125
[12] Gilibert M, Giménez X, Huarte-Larrañaga F, González M, Aguilar A, Last I and Baer M 1999 *J. Chem. Phys.* **110** 6278
[13] Gilibert M, Blasco R M, González M, Giménez X, Aguilar A, Last I and Baer M 1997 *J. Phys. Chem.* A **101** 6821
[14] Kress J D, Walker R B, Hayes E F and Pendergast P 1994 *J. Chem. Phys.* **100** 2728
[15] Pendergast P, Heck J M, Hayes E F and Jaquet R 1993 *J. Chem. Phys.* **98** 4543, and references therein
[16] Urban J, Klimo V, Staemmler V and Jaquet R 1991 *Z. Phys.* D: *At. Mol. Clusters* **21** 329
[17] Urban J, Jaquet R and Staemmler V 1990 *Int. J. Quantum Chem.* **38** 339
[18] Hayes E F, Siu A K Q, Chapman F M and Matcha R L 1976 *J. Chem. Phys.* **65** 1901
[19] Kuntz P J and Roach A C 1972 *J. Chem. Soc. Faraday Trans.* **68** 259
[20] Polanyi J C and Wong W H 1969 *J. Chem. Phys.* **51** 1439
[21] Zhang X and Han K L 2006 *Int. Quantum Chem.* **106** 1815
[22] Li R J, Han K L, Li F E, Lu R C, He G Z and Lou N Q 1994 *Chem. Phys. Lett.* **220** 281
[23] Han K L, He G Z and Lou N Q 1996 *J. Chem. Phys.* **105** 8699, and references therein
[24] Han K L, Zheng X G, Sun B F, He G Z and Zhang R Q 1991 *Chem. Phys. Lett.* **181** 474
[25] Liu S L and Shi Y 2011 *Chin. Phys.* B **20** 013404
[26] Han B R, Zong F J, Wang C L, Ma W Y and Zhou J H 2010 *Chem. Phys.* **374** 94
[27] Ge M H and Zheng Y J 2011 *Theor. Chem. Acc.* **129** 173
[28] Kong H, Liu X G, Xu W W, Liang J J and Zhang Q G 2009 *Acta Phys. Sin.* **58** 6926 (in Chinese)
[29] Xu Y, Zhao J, Yue D G, Zheng X Y and Meng Q T 2009 *Chin. Phys.* B **18** 5308
[30] Zhao J, Xu Y and Meng Q T 2010 *Chin. Phys.* B **19** 063403
[31] Hartree W S, Simons J P and Gonzalez-Urena A 1990 *J. Chem. Soc. Faraday Trans.* **86** 17
[32] Prisant M G, Rettner C T and Zare R N 1984 *J. Chem. Phys.* **81** 2699
[33] Chu T S 2010 *J. Comput. Chem.* **31** 1385
[34] Li B and Han K L 2009 *J. Phys. Chem.* A **113** 10189
[35] Ju L P, Han K L and Zhang J Z H 2009 *J. Comput. Chem.* **30** 305
[36] Varandas A J C 2000 *Int. Rev. Phys. Chem.* **19** 199